Advances in Fluid, Heat and Materials Engineering

Journal homepage:
https://karyailham.com.my/index.php/afhme/index
ISSN: 3083-8134

Investigation of Component Structure Materials for the Development of a Small-Scale Wing-in-Ground Effect (WIG) Craft

Ahmad Zuhairi Aszman [1], Siti Juita Mastura Mohd Saleh[2*]

[1] Department of Mechanical Engineering, Faculty of Mechanical and Manufacturing Engineering, Universiti Tun Hussein Onn Malaysia
[2] Department of Aeronautical Engineering, Faculty of Mechanical and Manufacturing Engineering, Universiti Tun Hussein Onn Malaysia

ARTICLE INFO

Article history:
Received 9 December 2024
Received in revised form 16 December 2024
Accepted 17 December 2024
Available online 31 December 2024

Keywords:
WIG craft materials; Wing-in-Ground (WIG) effect; ground effect vehicles; WIG craft fabrication

ABSTRACT

A Wing-in-Ground Effect (WIG) craft is a vehicle resembling an aircraft that operates using the ground effect phenomenon. This phenomenon occurs when lift force is enhanced as the craft's wings glide close to the earth's surface, either water or ground within a two-meter height boundary. Although well-documented in aeronautics, the fabrication of WIG crafts remains in its early stages, with limited research on the materials suitable for constructing these hybrid air-ground vehicles. This research investigates the mechanical performance of four materials for WIG craft components: Carbon Fiber Reinforced Polymer (CFRP), Glass Fiber Reinforced Polymer (GFRP), aluminum alloy 7075-T6, and Inconel 718 alloy. Using SolidWorks Simulation software, static tests were performed to evaluate stress, strain, and displacement across key components, including the fuselage, wings, engine mount, and tail structures. The results revealed that CFRP, with its exceptional strength-to-weight ratio, is the most suitable material for the fuselage and wings, ensuring structural integrity and aerodynamic efficiency. Aluminum alloy 7075-T6 was selected for the horizontal and vertical tail structures due to its strength and durability. Inconel 718 alloy, with its superior resistance to high temperatures and mechanical stress, was identified as the optimal material for the engine mount. These findings establish a practical framework for material selection in WIG craft development. Recommendations for future research include exploring alternative materials, optimising component design, and conducting experimental validations to enhance the robustness and efficiency of WIG craft fabrication.

1. Introduction

1.1 Background

Wing-in-Ground Effect (WIG) vehicles, commonly known as WIG crafts, are defined as vehicles resembling airplanes that utilise the ground effect. They feature wings attached to the main body, known in the aviation industry as the fuselage. When the wings glide near the earth's surface,

* *Corresponding author.*
E-mail address: juita@uthm.edu.my

https://doi.org/10.37934/afhme.3.1.4253a

whether over land or water within a boundary of approximately two meters in height, the lift force is significantly enhanced by the phenomenon known as the ground effect [1].

Despite the numerous advantages and promising potential of WIG craft technology, its development remains incomplete. Only a limited number of companies are currently involved in producing WIG crafts, with production levels remaining minimal. A significant contributing factor is the lack of standardised research on materials specifically suited for WIG crafts. Most companies rely on materials used by predecessors or competitors rather than conducting independent research to identify optimal materials. Furthermore, the limited number of academic studies on this topic has slowed the progress of WIG craft technology [2-4].

1.2 Materials for WIG Structure

To thoroughly identify the most suitable materials for the main components of a WIG craft, specifically the fuselage, wings, and tailplane, several aspects must be carefully considered. These include the operational characteristics of the craft, environmental exposure during motion, operational procedures that impact the structure, and other relevant factors that require detailed evaluation [5]. Selecting the right materials is crucial to ensure optimal performance, safety, and longevity of the craft. Factors such as mechanical properties, fatigue resistance, weight efficiency, and environmental durability must all be assessed to match the unique demands of WIG craft operation.

The primary materials used for WIG craft components include carbon fiber reinforced plastic (CFRP), glass-fiber reinforced plastic (GFRP), and aluminum alloys. Korea Ocean Research & Development Institute (KORDI) has extensively studied WIG crafts, producing various models categorised by seat capacity and scale. Research on the structural configuration of a six-seat small-scale WIG craft revealed a heavy reliance on CFRP. Carbon/Epoxy in a unidirectional (UD) configuration was utilised for wing spar flanges, fuselage stringers, and ring frames, while the same material in a fabric form was used for fuselage skins [6-9].

The Seafalcon, a WIG craft classified under Dynamic Air Cushion Craft (DACC), was first developed by German researchers in 1997. Originally a two-seater craft, it expanded to an eight-seater model by 2014, following successful trials. Since 2003, the Seafalcon has employed full-sized GFRP, leveraging its favourable properties [10]. However, despite its high tensile strength, GFRP has limitations, including insufficient stiffness and rigidity for certain structural applications. Additionally, fiberglass-based materials are restricted in operations above 200^0C due to the low heat resistance of most polymer matrices, except for polyimide resins [9,11].

A study by Swetha and Gundlathoti [12] analysed the structural design and fatigue of a Power Augmented Ram Wing-in-Ground (PARWIG) craft, a WIG craft variant. The PARWIG was designed as a small-scale craft for a single passenger, with loads applied to its wings, fuselage, and horizontal tail. Aluminum alloys, particularly those enhanced with magnesium and zinc, such as aluminum-zinc 7010-T7451, showed increased strength due to heat treatment. However, excessive magnesium and zinc content can reduce overall corrosion resistance, including stress and exfoliation corrosion. The inclusion of copper in the alloy improves strength and stress corrosion resistance, making it one of the strongest commercially available aluminum-based alloys in the 7XXX series [13-18].

This research is conducted to fill the gap in knowledge regarding materials used in the construction of WIG craft components, providing essential insights to support future advancements in this field.

2. Methodology

2.1 WIG Craft CAD Model

As the initial step, the WIG craft model was designed using SolidWorks software, as illustrated in Figure 1.

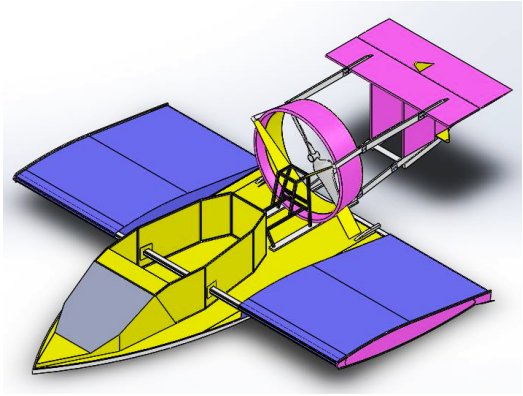

Fig. 1. The WIG craft model

2.2 Material Selection

In this research, four types of materials were considered: CFRP, GFRP, aluminum-zinc 7075-T6, and Inconel 718 alloy. The selection of these materials is based on three different types of WIG craft; WIG, PARWIG, and DACC [11]. Inconel 718 alloy, a chromium-based alloy, was included due to its high resistance to temperature. These materials were selected from previous studies by Bandaru Swetha and Gundlathoti [12], business brochures from companies such as HOVERWING 80, AirFish-8, and WSH-500, as well as material property charts, including young's modulus versus density chart [18], fracture toughness versus young's modulus chart [18], strength versus density chart [18], strength versus maximum service temperature chart [18], and the S-N curve [19-21].

2.3 SolidWorks Static Test Simulation

All materials analysed in SolidWorks Simulation undergo a static test, with connection sets verified prior to running the simulation. Preparations for the static test involved applying fixtures, external loads, and meshing. The fixtures were designed to restrain the parts, to ensure no movement under applied forces. Their application was based on guidelines from the journal Structural Design and Fatigue Analysis of a WIG (Wing-in-Ground) Vehicle [12]. The static test simulation is then conducted to obtain the results for maximum stress, maximum strain, and displacement for each material and component structure.

2.3.1 Fixtures

The fixtures for the structural components are shown in Figures 2 to 6, corresponding to the wing, fuselage, engine mount, horizontal tail, and vertical tail, respectively. Subsequently, a static test simulation is conducted to determine the maximum stress, maximum strain, and displacement for each structural component, with results analysed for each material used.

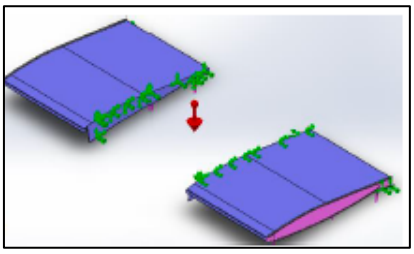

Fig. 2. Fixtures for wing

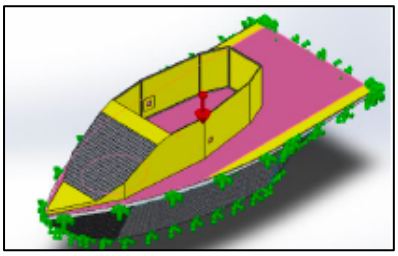

Fig. 3. Fixtures for fuselage

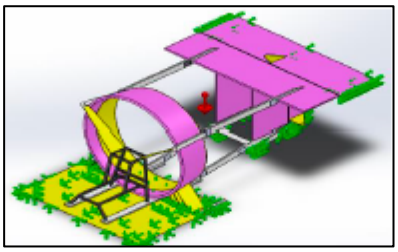

Fig. 4. Fixtures for engine mount

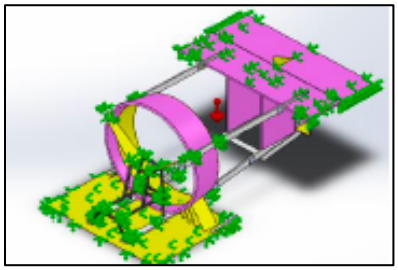

Fig. 5 Fixtures for horizontal tail

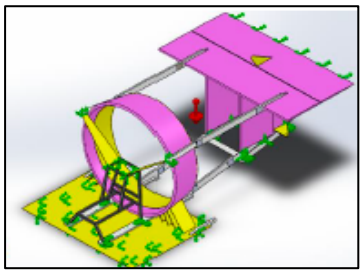

Fig. 6 Fixtures for vertical tail

2.3.2 External Loads

External loads are applied once the fixtures are correctly implemented on the parts of the WIG craft model. These loads represent the forces acting on the model during motion, including gravity, which is applied to each component. The loads, based on the reference, are applied accordingly, considering the different design of the model. The external loads applied to the component structures are detailed in Tables 1 to 5, corresponding to the wing, fuselage, engine mount, horizontal tail, and vertical tail, respectively.

Table 1
External loads for wing

Load name	Load details	
Force 1	Entities	4 faces
	Type	Normal force
	Value	19.62 N
Gravity 1	Reference	Top plane
	Value	-9.81
	Unit	SI

Table 2
External loads for fuselage

Load name	Load details	
Force 1	Entities	2 faces
	Type	Normal force
	Value	2.6 N
Force 2	Entities	9 faces
	Type	Normal force
	Value	19.62 N
Force 3	Entities	1 face
	Type	Normal force
	Value	0.8 N

Gravity 1	Reference	Top plane
	Value	-9.81
	Unit	SI

Table 3
External loads for engine mount

Load name	Load details	
Force 1	Entities	18 faces
	Type	Normal force
	Value	3.924 N
Gravity 1	Reference	Top plane
	Value	-9.81
	Unit	SI

Table 4
External loads for horizontal tail

Load name	Load details	
Force 1	Entities	4 faces
	Type	Normal force
	Value	3.924 N
Gravity 1	Reference	Top plane
	Value	-9.81
	Unit	SI

Table 5
External loads for vertical tail

Load name	Load details	
Force 1	Entities	20 faces
	Type	Normal force
	Value	3.924 N
Gravity 1	Reference	Top plane
	Value	-9.81
	Unit	SI

2.3.3 Mesh

All components in this research were meshed using the blended curvature-based option to accommodate the intricate designs, with varying element sizes detailed in Figures 7 to 9.

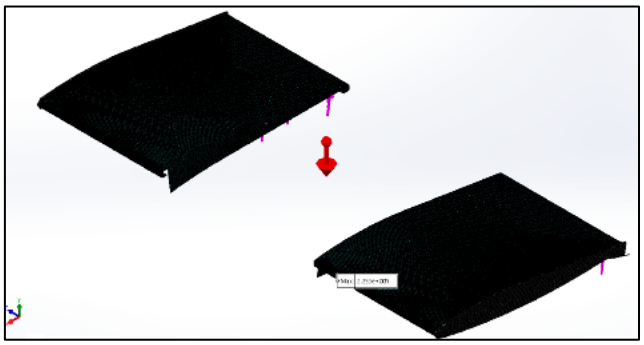

Fig. 7. Meshing at wing component

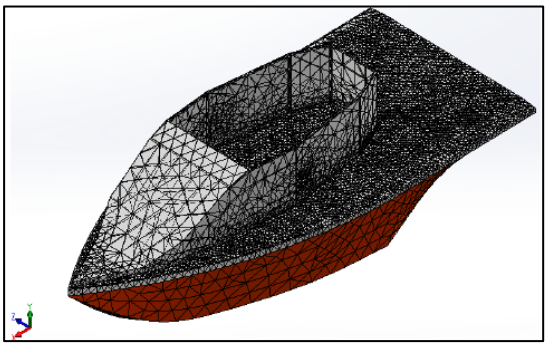

Fig. 8. Fixtures for fuselage

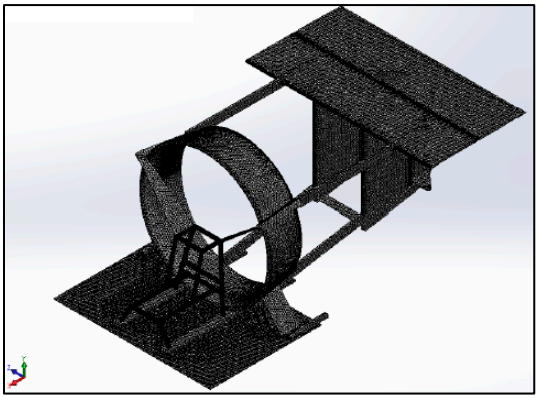

Fig. 9. Fixtures for engine mount

3. Results

3.1 Fatigue (SN-Curve)

The S-N curves for CFRP, GFRP, aluminum alloy 7075-T6, and Inconel 718 alloy are presented in Figure 10. CFRP exhibited the highest fatigue life, sustaining maximum stress levels of 700 MPa at 10^1 cycles and 400 MPa at 10^6 cycles before the onset of microcracks. In contrast, GFRP demonstrated fatigue failure at stress levels below 100 MPa after only 10^1 cycles. While initially comparable to aluminum alloy 7075-T6, Inconel 718 alloy exhibited fatigue at 300 MPa for cycles exceeding 10^2, indicating faster degradation under repeated stresses. CFRP showed a 57% to 71% higher stress resistance compared to aluminum alloy 7075-T6 and Inconel 718 alloy, establishing it as the superior material for fatigue resistance.

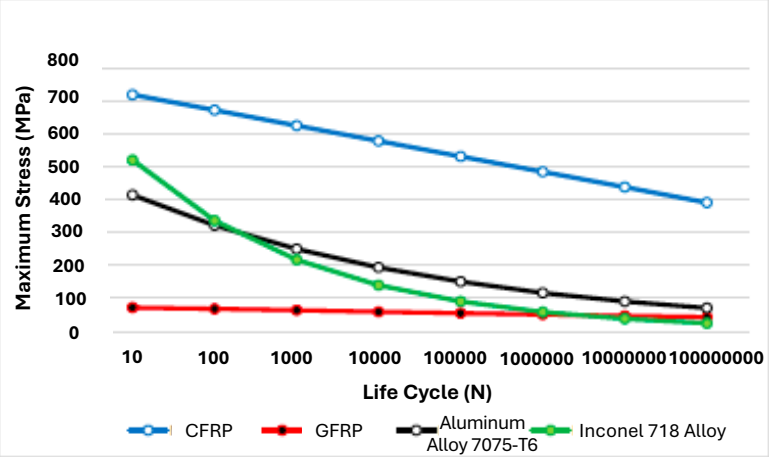

Fig. 10. SN-Curve the selected materials

3.2 Wing

The example results for principal stress on the wing using CFRP material is shown in Figure 11. The maximum principal stress, strain, and displacement results for all materials are illustrated in Figure 12, Figure 13, and Figure 14, respectively. From Figure 12, the maximum principal stress on the wings of the WIG craft model is 45100 MPa. Inconel 718 alloy displayed the highest value for maximum principal stress, while CFRP and GFRP exhibited the lowest values for maximum stress, respectively. The maximum strain values presented in Figure 13 reveal that CFRP had the lowest

strain at 0.04, while Inconel 718 alloy displayed the highest strain at 0.28. GFRP and aluminum alloy 7075-T6 exhibited intermediate strain values of 0.25and 0.21, respectively.

Maximum resultant displacement in Figure 14 showed that CFRP at 272 mm, the lowest among materials. Inconel 718 alloy displayed 1807 mm, GFRP measured 1545 mm, and aluminum alloy 7075-T6 recorded 1371 mm, indicating greater rigidity of CFRP under load.

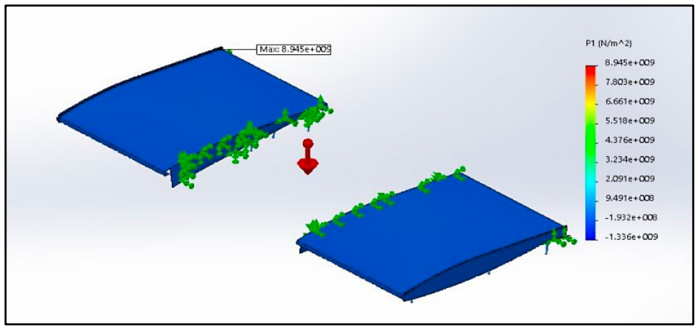

Fig. 11. Example of maximum principal stress result for CFRP on wings

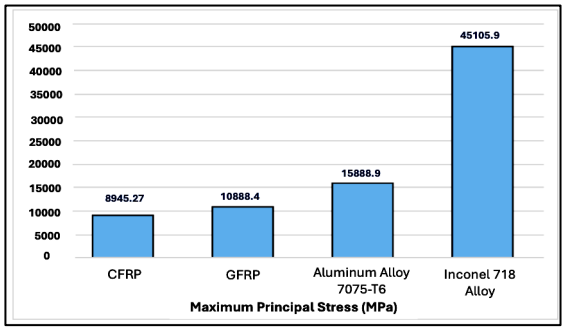

Fig. 12. Result of maximum principal stress for all materials on wing structure

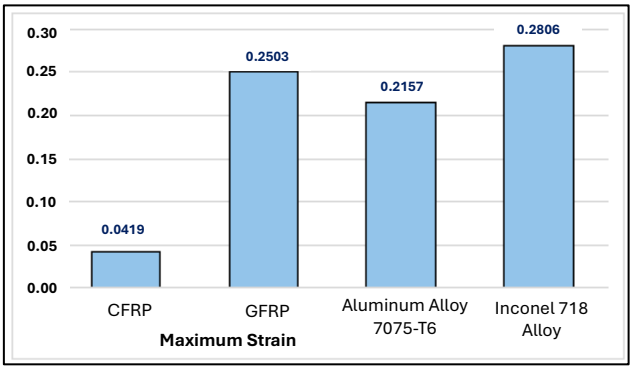

Fig. 13. Results of maximum strain for all materials on wing structure

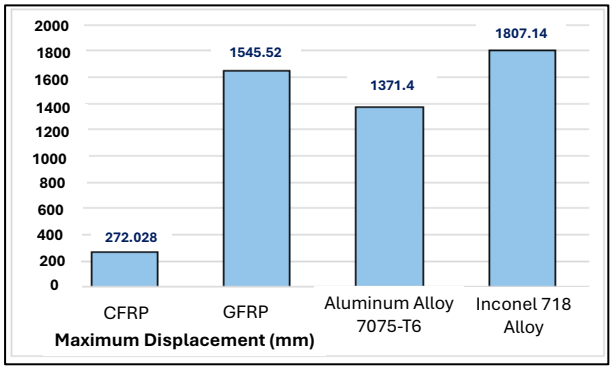

Fig. 14. Results of maximum displacement for all materials on wing structure

3.3 Fuselage

The example results for principal stress on the fuselage using CFRP material is shown in Figure 15. The maximum principal stress, strain, and displacement results for all materials are provided in Figure 16, Figure 17, and Figure 18, respectively.

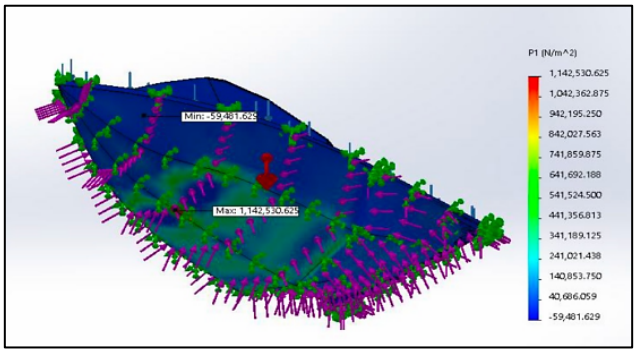

Fig. 15. Example of maximum principal stress result for CFRP on fuselage

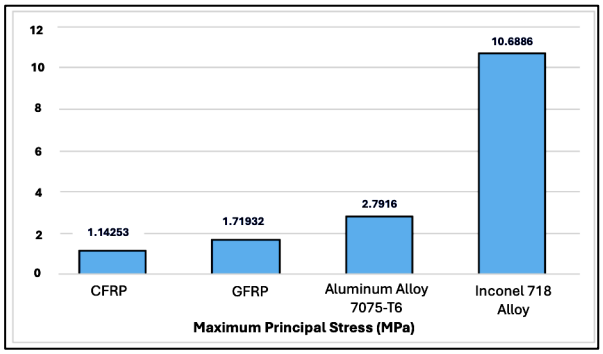

Fig. 16. Result of maximum principal stress for all materials on fuselage structure

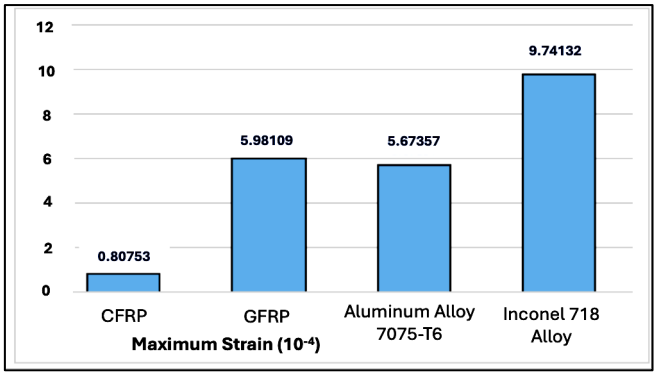

Fig. 17. Results of maximum strain for all materials on fuselage structure

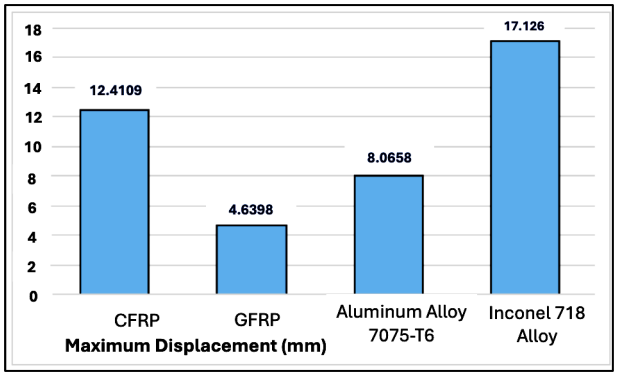

Fig. 18. Results of maximum displacement for all materials on fuselage structure

From Figure 16, the maximum principal stress for the fuselage using Inconel 718 alloy is 10 MPa, the highest among tested materials, while CFRP had the lowest at 1.14 MPa. GFRP and aluminum alloy 7075-T6 exhibited 1.72 MPa and 2.79 MPa, respectively. The maximum strain values in Figure 17 shows that Inconel 718 alloy with the highest strain at 9.74×10^{-4}, while CFRP recorded 8.08×10^{-5}, the lowest. GFRP and aluminum alloy 7075-T6 show strain values of 5.98×10^{-4} and 5.67×10^{-4}, respectively. Maximum displacement results in Figure 18 for GFRP were the lowest at 4.6 mm, while Inconel 718 Alloy exhibited the highest at 17.1 mm. GFRP showed minimal displacement, highlighting its stiffness.

3.4 Engine Mount

The example results for principal stress on the engine mount using CFRP material is shown in Figure 19. The maximum principal stress, strain, and displacement results for all materials are shown in Figure 20, Figure 21, and Figure 22, respectively. Inconel 718 alloy recorded the highest maximum principal stress of 18.8 MPa at the engine mount (Figure 20), while CFRP and GFRP showed almost similar values around 4 MPa. Aluminum alloy 7075-T6 shows the highest value of 6.48 MPa, reflecting its moderate stress-handling capability.

Figure 21 shows CFRP with the lowest strain at 1.09×10^{-5}, while Inconel 718 alloy had the highest at 7.22×10^{-5}. Aluminum alloy 7075-T6 and GFRP had strain values of $5.74\times10^{-5}$and 6.38×10^{-5}, respectively. In Figure 22, CFRP demonstrated the lowest displacement of 5.34×10^{-6} mm, while Inconel 718 alloy exhibited the highest at 22.62×10^{-6} mm. GFRP and aluminum alloy 7075-T6 recorded 6.67×10^{-6} mm and 8.67×10^{-6} mm, respectively

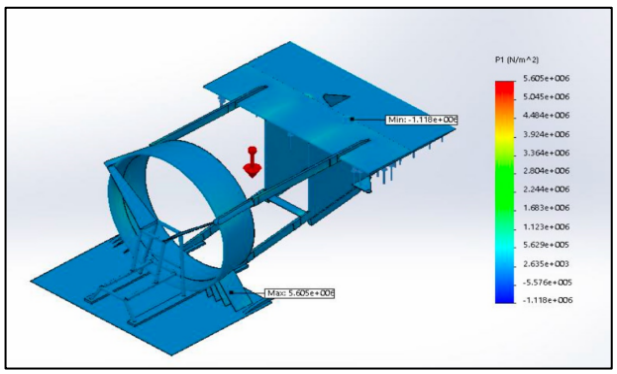

Fig. 19. Example of maximum principal stress result for CFRP on engine mount

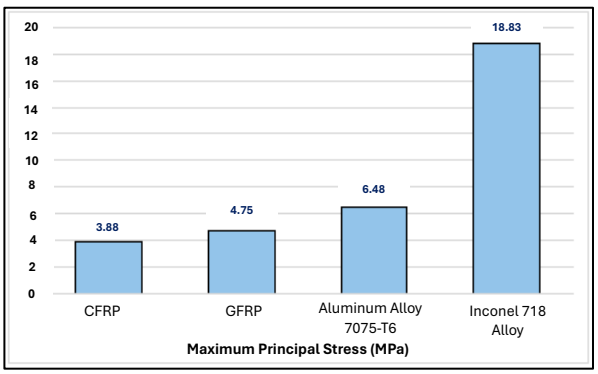

Fig. 20. Result of maximum principal stress for all materials on engine mount

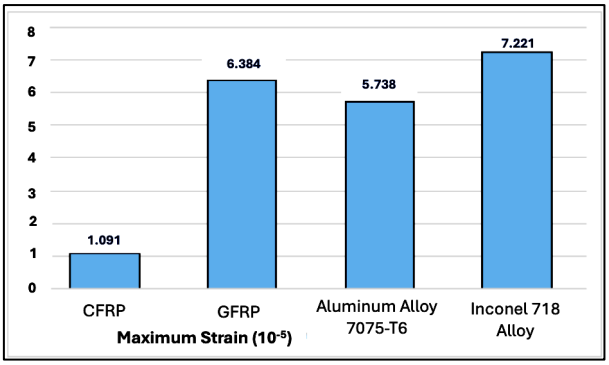

Fig. 21. Results of maximum strain for all materials on engine mount

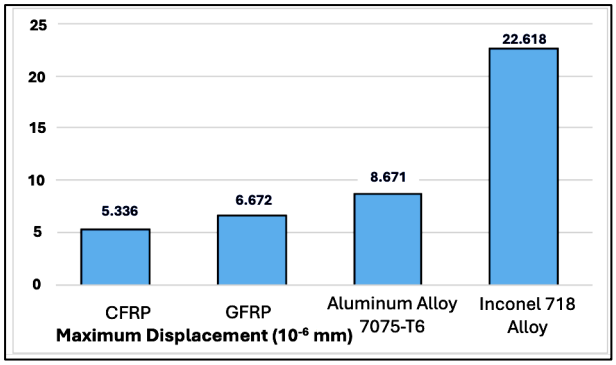

Fig. 22. Results of maximum displacement for all materials on engine mount

3.5 Tailplane

3.5.1 Horizontal tail

The example results for principal stress on the horizontal tail using CFRP material is shown in Figure 23. The maximum principal stress, strain, and displacement results for all materials are displayed in Figure 24, Figure 25, and Figure 26, respectively.

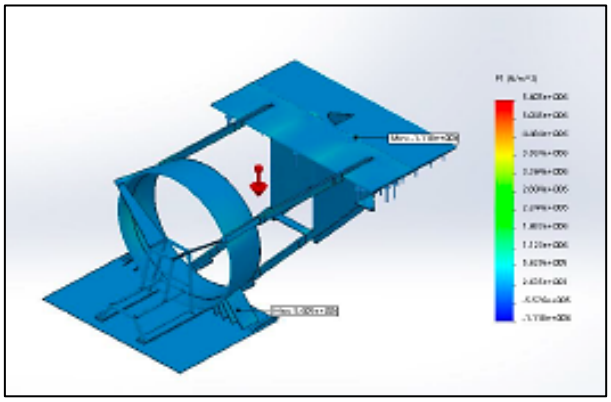

Fig. 23. Example of maximum principal stress result for CFRP on horizontal tail

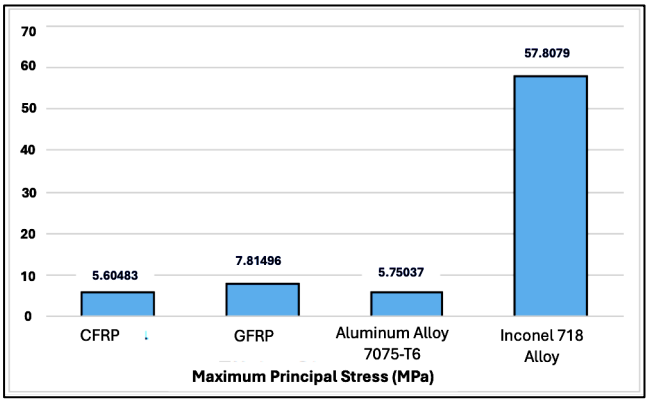

Fig. 24. Result of maximum principal stress for all materials on horizontal tail

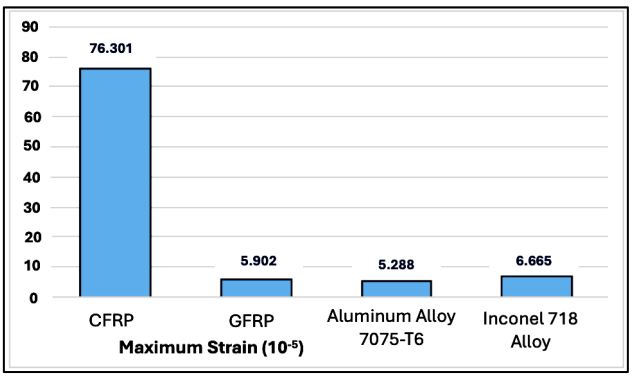

Fig. 25. Results of maximum strain for all materials on horizontal tail

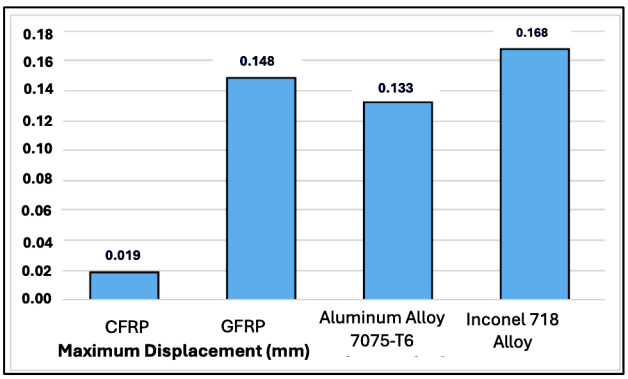

Fig. 26. Results of maximum displacement for all materials on horizontal tail

Figure 24 shows maximum principal stress values of 5.7 MPa for both CFRP and aluminum alloy 7075-T6, the lowest among tested materials. Inconel 718 alloy exhibited 57 MPa, while GFRP recorded 7.8 MPa. CFRP exhibited the highest strain value of 76.3×10^{-5} (Figure 25), while aluminum

alloy 7075-T6 had the lowest at 5.2×10^{-5}. GFRP and Inconel 718 alloy showed strain values of $5.9\times10^{-5}$and 6.7×10^{-5}, respectively. Maximum resultant displacement values in Figure 26 reveal CFRP at 0.019 mm, the lowest, with Inconel 718 alloy at 0.168 mm, the highest. Aluminum alloy 7075-T6 and GFRP were closer at 0.148 mm and 0.133 mm, respectively.

3.5.2 Vertical tail

The example results for principal stress on the vertical tail using CFRP material is shown in Figure 27. The maximum principal stress, strain, and displacement results for all materials are displayed in Figure 28, Figure 29, and Figure 30, respectively. Figure 28 shows Inconel 718 alloy recorded 64.17 MPa, the highest maximum principal stress. CFRP exhibited 13.26 MPa, the lowest. Aluminum alloy 7075-T6 and GFRP demonstrated values of 23.05 MPa and 16.31 MPa, respectively.

In Figure 29, CFRP again displayed the highest strain at 72.28×10^{-4}, while aluminum alloy 7075-T6 recorded the lowest at 3.89×10^{-4}. GFRP and Inconel 718 alloy recorded strain values of 4.14×10^{-4} and 4.82×10^{-4}, respectively. CFRP demonstrated the lowest displacement at 0.34 mm (Figure 30), with Inconel 718 alloy showing the highest at 2.19 mm. GFRP and aluminum alloy 7075-T6 had displacement values of 2.01 mm and 1.71 mm, respectively.

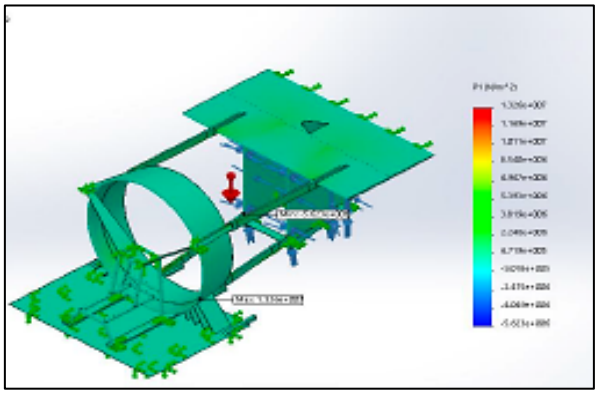

Fig. 27. Example of maximum principal stress result for CFRP on vertical tail

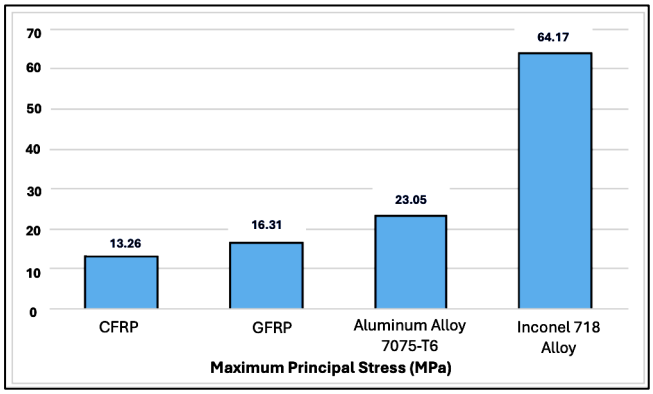

Fig. 28. Result of maximum principal stress for all materials on vertical tail

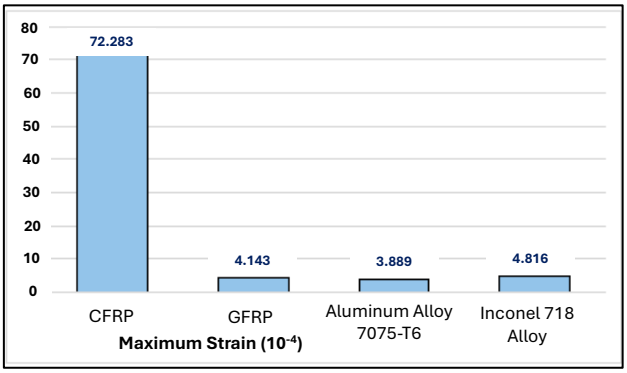

Fig. 29. Results of maximum strain for all materials on vertical tail

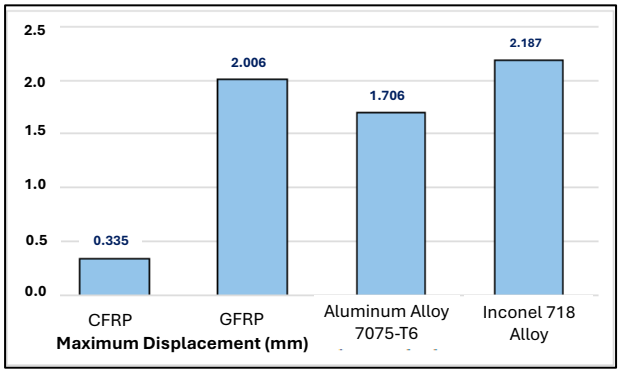

Fig. 30. Results of maximum displacement for all materials on vertical tail

4. Conclusions

CFRP emerged as the most reliable material due to its superior stiffness, minimal deformation, and exceptional fatigue resistance. Its ability to sustain maximum stress levels of 700 MPa

at 10^1 cycles and 400 MPa at 10^6 cycles, coupled with the lowest strain and displacement values, shows its suitability for critical components. Consequently, CFRP is the ideal choice for the fuselage and wings, where a high strength-to-weight ratio is essential for enhancing aerodynamic performance and fuel efficiency. Inconel 718 alloy demonstrated excellent stress-handling capabilities and high-temperature resistance, making it optimal for the engine mount, which is subject to extreme thermal and mechanical loads. However, its higher strain and displacement values limit its application in components requiring high rigidity. GFRP and aluminum alloy 7075-T6 exhibited moderate performance, with GFRP showing minimal displacement and aluminum alloy 7075-T6 offering a balance of strength and durability. These characteristics make them suitable for less critical structural parts, such as the horizontal and vertical tail structures, where performance demands are less stringent. These findings provide a strong foundation for material selection in WIG craft development, ensuring an optimal balance of performance, weight, and durability. Future research should explore advanced composite materials, refine component designs, and incorporate experimental validations to further improve WIG craft efficiency and reliability.

Acknowledgement
This research was not funded by any grant.

References

[1] Kong, C., H. Park, Y. Kim, and K. Kang. "Structural design on wing of a small scale wig vehicle with carbon/epoxy and foam sandwich composite structure." In *16th International Conference on Composite Materials*, p. 1-8. 2007.
[2] Pua'at, Afifi A., Amzari Zhahir, Mohamed Tarmizi Ahmad, and Aziz Hassan. "Review on the Development of Wing-In-Ground Crafts." In *E3S Web of Conferences* 477, p. 00010. EDP Sciences, 2024. https://doi.org/10.1051/e3sconf/202447700010
[3] Yang, Wei, and Paul A. Czysz. "WIG craft serves niche transportation needs." *World Review of Intermodal Transportation Research* 3, no. 4 (2011): 395-406. https://doi.org/10.1504/WRITR.2011.041720
[4] Halloran, Michael, and Sean O'Meara. *Wing in ground effect craft review*. Australia: DSTO Aeronautical and Maritime Research Laboratory, 1999.
[5] Abidin, Razali, Mohamad Asmidzam Ahamat, Tarmizi Ahmad, Mohd Rasdan Saad, and Ezzat Hafizi. "Preliminary development of a wing in ground effect vehicle." In *AIP Conference Proceedings*, 1930, no. 1. AIP Publishing, 2018. https://doi.org/10.1063/1.5022898
[6] Rozhdestvensky, Kirill V. "Wing-in-ground effect vehicles." *Progress in Aerospace Sciences* 42, no. 3 (2006): 211-283. https://doi.org/10.1016/j.paerosci.2006.10.001
[7] Nebylov, Alexander. "Wing-In-Ground Vehicles: Modern Concepts of Design, Automatic Control, Applications." *State University of Aerospace Instrumentation, Saint-Petersburg, Russia* (2006). https://doi.org/10.1063/1.5022898
[8] Chung, Deborah DL. *Applied materials science: applications of engineering materials in structural, electronics, thermal, and other industries*. CRC Press, 2001. https://doi.org/10.1201/9781420040975
[9] Callister Jr, William D., and David G. Rethwisch. *Materials science and engineering: an introduction*. John wiley & sons, 2020.
[10] Hameed, Hassan. "The design of a four-seat reverse delta WIG craft." (2019). https://doi.org/10.62338/8nsr3z50
[11] Askeland, Donald R., P. P. Fulay, and W. J. Wright. "The science and engineering of materials 6th edition." *Cengage Learning Inc* 889 (2010).
[12] Swetha, B. Sowmya, and Gundlathoti Sowmya. "G. Structural design and fatigue analysis of a WIG (Wing in Ground) vehicle." *International Journal of Latest Trends in Engineering and Technology (IJLTET)* (2013).
[13] Prasad, N. Eswara, and Russel JH Wanhill, eds. *Aerospace materials and material technologies*. Vol. 1. Singapore: Springer, 2017. https://doi.org/10.1007/978-981-10-2143-5
[14] Barnhart, Joel. "Occurrences, uses, and properties of chromium." *Regulatory toxicology and pharmacology* 26, no. 1 (1997): S3-S7. https://doi.org/10.1006/rtph.1997.1132
[15] Lunk, Hans-Joachim, and Hans Hartl. "Discovery, properties and applications of molybdenum and its compounds." *ChemTexts* 3 (2017): 1-23. https://doi.org/10.1007/s40828-017-0048-6

[16] Locq, D., P. Caron, C. Ramusat, and R. Mévrel. "Quaternary chromium-based alloys strengthened by Heusler phase precipitation." *Materials Science and Engineering: A* 647 (2015): 322-332. https://doi.org/10.1016/j.msea.2015.09.033
[17] Gu, Y. F., H. Harada, and Y. Ro. "Chromium and chromium-based alloys: Problems and possibilities for high-temperature service." *Jom* 56 (2004): 28-33. https://doi.org/10.1007/s11837-004-0197-0
[18] Design, Granta. *Material and process selection charts*. 2010.
[19] Pradeep Kumar, Pranav. "From fatigue-to-fracture: Probabilistic total-life of steel bridge structures." *PhD diss.*, 2022.
[20] Murakami, Yukitaka, Toshio Takagi, Kentaro Wada, and Hisao Matsunaga. "Essential structure of SN curve: Prediction of fatigue life and fatigue limit of defective materials and nature of scatter." *International Journal of Fatigue* 146 (2021): 106138. https://doi.org/10.1016/j.ijfatigue.2020.106138
[21] Burhan, Ibrahim, and Ho Sung Kim. "SN curve models for composite materials characterisation: an evaluative review." *Journal of Composites Science* 2, no. 3 (2018): 38. https://doi.org/10.3390/jcs2030038